Transformers without Normalization

Jiachen Zhu[1,2], **Xinlei Chen**[1], **Kaiming He**[3], **Yann LeCun**[1,2], **Zhuang Liu**[1,4,†]

[1]FAIR, Meta, [2]New York University, [3]MIT, [4]Princeton University
[†]Project lead

Normalization layers are ubiquitous in modern neural networks and have long been considered essential. This work demonstrates that Transformers without normalization can achieve the same or better performance using a remarkably simple technique. We introduce Dynamic Tanh (DyT), an element-wise operation $\mathrm{DyT}(\boldsymbol{x}) = \tanh(\alpha \boldsymbol{x})$, as a drop-in replacement for normalization layers in Transformers. DyT is inspired by the observation that layer normalization in Transformers often produces tanh-like, S-shaped input-output mappings. By incorporating DyT, Transformers without normalization can match or exceed the performance of their normalized counterparts, mostly without hyperparameter tuning. We validate the effectiveness of Transformers with DyT across diverse settings, ranging from recognition to generation, supervised to self-supervised learning, and computer vision to language models. These findings challenge the conventional understanding that normalization layers are indispensable in modern neural networks, and offer new insights into their role in deep networks.

Date: March 14, 2025
Project page and code: jiachenzhu.github.io/DyT
Correspondence: jiachen.zhu@nyu.edu, zhuangl@princeton.edu

1 Introduction

Over the past decade, normalization layers have solidified their positions as one of the most fundamental components of modern neural networks. It all traces back to the invention of batch normalization in 2015 (Ioffe and Szegedy, 2015), which enabled drastically faster and better convergence in visual recognition models and quickly gained momentum in the following years. Since then, many variants of normalization layers have been proposed for different network architectures or domains (Ba et al., 2016; Ulyanov et al., 2016; Wu and He, 2018; Zhang and Sennrich, 2019). Today, virtually all modern networks use normalization layers, with layer normalization (Layer Norm, or LN) (Ba et al., 2016) being one of the most popular, particularly in the dominant Transformer architecture (Vaswani et al., 2017; Dosovitskiy et al., 2020).

The widespread adoption of normalization layers is largely driven by their empirical benefits in optimization (Santurkar et al., 2018; Bjorck et al., 2018). In addition to achieving better results, they help accelerate and stabilize convergence. As neural networks become wider and deeper, this necessity becomes ever more critical (Brock et al., 2021a; Huang et al., 2023). Consequently, normalization layers are widely regarded as crucial, if not indispensable, for the effective training of deep networks. This belief is subtly evidenced by the fact that, in recent years, novel architectures often seek to replace attention or convolution layers (Tolstikhin et al., 2021; Gu and Dao, 2023; Sun et al., 2024; Feng et al., 2024), but almost always retain the normalization layers.

This paper challenges this belief by introducing a simple alternative to normalization layers in Transformers. Our exploration starts with the observation that LN layers map their inputs to outputs with tanh-like, S-shaped curves, scaling the input activations while squashing the extreme values. Inspired by this insight, we propose an element-wise operation termed Dynamic Tanh (DyT), defined as: $\mathrm{DyT}(\boldsymbol{x}) = \tanh(\alpha \boldsymbol{x})$, where α is a learnable parameter. This operation aims to emulate the behavior of LN by learning an appropriate scaling factor through α and squashing extreme values via the bounded tanh function. Notably, unlike normalization layers, it achieves both effects without the need to compute activation statistics.

Employing DyT is straightforward, as shown in Figure 1: we directly replace existing normalization layers with DyT in architectures such as vision and language Transformers. We empirically demonstrate that models with DyT can train stably and achieve high final performance across a wide range of settings. It often does not

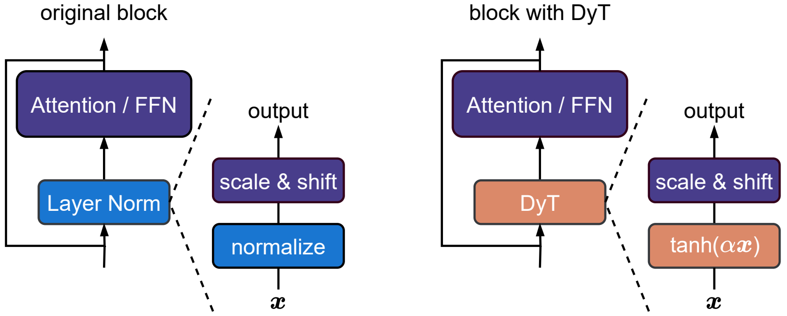

Figure 1 *Left:* original Transformer block. *Right:* block with our proposed Dynamic Tanh (DyT) layer. DyT is a straightforward replacement for commonly used Layer Norm (Ba et al., 2016) (in some cases RMSNorm (Zhang and Sennrich, 2019)) layers. Transformers with DyT match or exceed the performance of their normalized counterparts.

require tuning the training hyperparameters on the original architecture. This work challenges the notion that normalization layers are indispensable for training modern neural networks and provides empirical insights into the properties of normalization layers. Moreover, preliminary measurements suggest that DyT improves training and inference speed, making it a candidate for efficiency-oriented network design.

2 Background: Normalization Layers

We begin by reviewing the normalization layers. Most normalization layers share a common formulation. Given an input $\boldsymbol{x}$ with shape (B, T, C), where B is the batch size, T is the number of tokens, and C is the embedding dimension per token, the output is generally computed as:

(samples, tokens, and channels)

$$\text{normalization}(\boldsymbol{x}) = \boldsymbol{\gamma} * \left(\frac{\boldsymbol{x} - \boldsymbol{\mu}}{\sqrt{\boldsymbol{\sigma}^2 + \epsilon}} \right) + \boldsymbol{\beta} \tag{1}$$

where ϵ is a small constant, and $\boldsymbol{\gamma}$ and $\boldsymbol{\beta}$ are learnable vector parameters of shape $(C,)$. They are "scaling" and "shifting" affine parameters that allow the output to be in any range. The terms $\boldsymbol{\mu}$ and $\boldsymbol{\sigma}^2$ denote the mean and variance of the input. Different methods mainly differ in how these two statistics are computed. This results in $\boldsymbol{\mu}$ and $\boldsymbol{\sigma}^2$ having different dimensions, each with broadcasting applied during computation.

Batch normalization (BN) (Ioffe and Szegedy, 2015) is the first modern normalization layer, and it has been primarily used in ConvNet models (Szegedy et al., 2016; He et al., 2016; Xie et al., 2017). Its introduction represents a major milestone in deep learning architecture designs. BN computes the mean and variance across both the batch and token dimensions, specifically: $\mu_k = \frac{1}{BT}\sum_{i,j} x_{ijk}$ and $\sigma_k^2 = \frac{1}{BT}\sum_{i,j}\left(x_{ijk} - \mu_k\right)^2$. Other normalization layers popular in ConvNets, such as group normalization (Wu and He, 2018) and instance normalization (Ulyanov et al., 2016), were initially proposed for specialized tasks such as object detection and image stylization. They share the same overall formulation but differ in the axes and ranges over which the statistics are computed.

Layer normalization (LN) (Ba et al., 2016) and root mean square normalization (RMSNorm) (Zhang and Sennrich, 2019) are the major two types of normalization layers used in Transformer architectures. LN computes these statistics independently for each token in each sample, where $\mu_{ij} = \frac{1}{C}\sum_k x_{ijk}$ and $\sigma_{ij}^2 = \frac{1}{C}\sum_k \left(x_{ijk} - \mu_{ij}\right)^2$. RMSNorm (Zhang and Sennrich, 2019) simplifies LN by removing the mean-centering step and normalizing the input with $\mu_{ij} = 0$ and $\sigma_{ij}^2 = \frac{1}{C}\sum_k x_{ijk}^2$. Today, most modern neural networks use LN due to its simplicity and universality. Recently, RMSNorm has gained popularity, particularly in language models like T5 (Raffel et al., 2020), LLaMA (Touvron et al., 2023a,b; Dubey et al., 2024), Mistral (Jiang et al., 2023), Qwen (Bai et al., 2023; Yang et al., 2024), InternLM (Zhang et al., 2024; Cai et al., 2024) and DeepSeek (Liu et al., 2024; Guo et al., 2025). The Transformers we examine in this work all use LN, except that LLaMA uses RMSNorm.

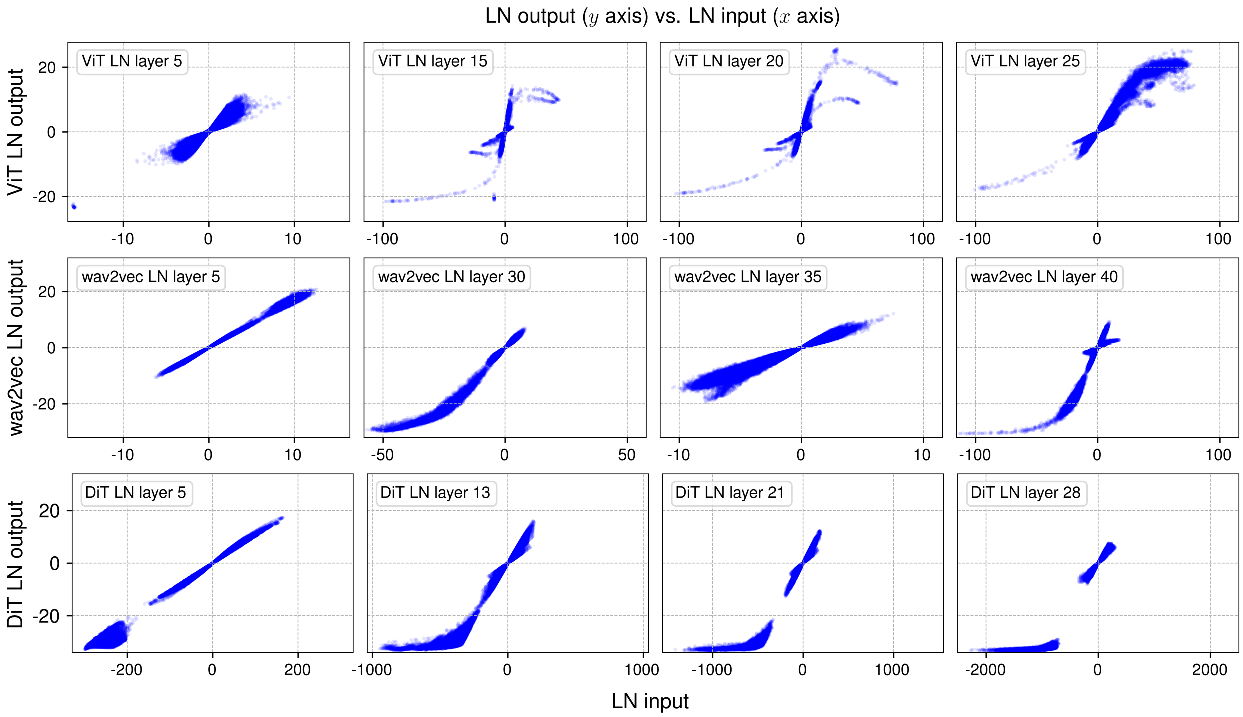

Figure 2 Output vs. input of selected layer normalization (LN) layers in Vision Transformer (ViT) (Dosovitskiy et al., 2020), wav2vec 2.0 (a Transformer model for speech) (Baevski et al., 2020), and Diffusion Transformer (DiT) (Peebles and Xie, 2023). We sample a mini-batch of samples and plot the input / output values of four LN layers in each model. The outputs are before the affine transformation in LN. The S-shaped curves highly resemble that of a tanh function (see Figure 3). The more linear shapes in earlier layers can also be captured by the center part of a tanh curve. This motivates us to propose Dynamic Tanh (DyT) as a replacement, with a learnable scaler α to account for different scales on the x axis.

3 What Do Normalization Layers Do?

Analysis setup. We first empirically study the behaviors of normalization layers in trained networks. For this analysis, we take a Vision Transformer model (ViT-B) (Dosovitskiy et al., 2020) trained on ImageNet-1K (Deng et al., 2009), a wav2vec 2.0 Large Transformer model (Baevski et al., 2020) trained on LibriSpeech (Panayotov et al., 2015), and a Diffusion Transformer (DiT-XL) (Peebles and Xie, 2023) trained on ImageNet-1K. In all cases, LN is applied in every Transformer block and before the final linear projection.

For all three trained networks, we sample a mini-batch of samples and do a forward pass through the network. We then measure the input and output for the normalization layers, i.e., tensors immediately before and after the normalization operation, before the learnable affine transformation. Since LN preserves the dimensions of the input tensor, we can establish a one-to-one correspondence between the input and output tensor elements, allowing for a direct visualization of their relationship. We plot the resulting mappings in Figure 2.

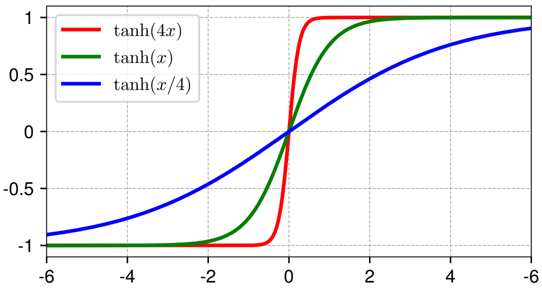

Figure 3 tanh(αx) with three different α values.

Tanh-like mappings with layer normalization. For all three models, in earlier LN layers (1st column of Figure 2), we find this input-output relationship to be mostly linear, resembling a straight line in an x-y plot. However, the deeper LN layers are places where we make more intriguing observations.

A striking observation from these deeper layers is that most of these curves' shapes highly resemble full or partial S-shaped curves represented by a tanh function (see Figure 3). One might expect LN layers to linearly transform the input tensor, as subtracting the mean and dividing by standard deviation are

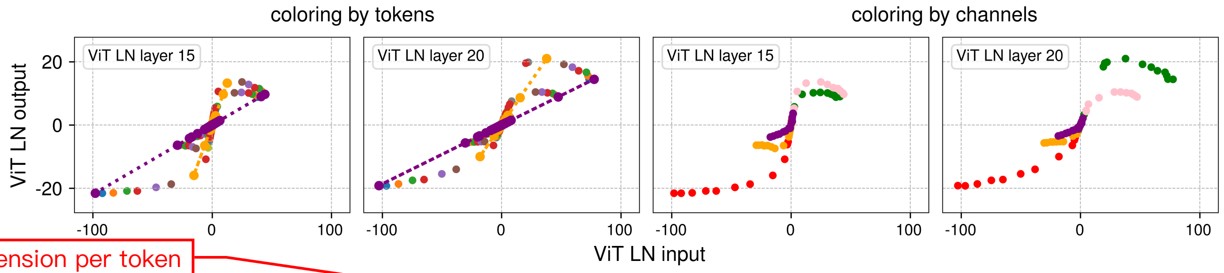

embedding dimension per token

e 4 Output vs. input of two LN layers, with tensor elements colored to indicate different channel and token dimensions. input tensor has a shape of (samples, tokens, and channels), with elements visualized by assigning consistent colors to the same tokens (left two panels) and channels (right two panels). *two panels*: points representing the same token (same color) form straight lines across different channels, as LN operates linearly across channels for each token. restingly, when plotted collectively, these lines form a non-linear tanh-shaped curve. *t two panels*: each channel's input spans different ranges on the x-axis, contributing distinct segments to the overall tanh-shaped curve. ain channels (e.g., red, green, and pink) exhibit more extreme x values, which are squashed by LN.

linear operations. normalizes in a per-token manner, only linearly transforming each token's activations. okens have different mean and standard deviation values, the linearity does not hold collectively on all activations of the input tensor. etheless, it is still surprising to us that the actual non-linear transformation is highly similar to a scaled tanh function.

such an S-shaped curve, we note that the central part, represented by points with x values close to zero, is still mainly in a linear shape. t points (∼99%) fall in this linear range. vever, there are still many points that clearly fall out of this range, which are considered to have "extreme" values, e.g., those with x larger than 50 or smaller than -50 in the ViT model. malization layers' main effect for these values is to *squash* them into less extreme values, more in line with the majority of points. s is where normalization layers could not approximated by a simple affine transformation layer. hypothesize this non-linear and disproportional squashing effect on extreme values is what makes normalization layers important and indispensable.

ent findings by Ni et al. (2024) similarly highlight the strong non-linearities introduced by LN layers, demonstrating how the non-linearity enhances a model's representational capacity. eover, this squashing behavior mirrors the saturation properties of biological neurons for large inputs, a phenomenon first observed about a century ago (Adrian, 1926; Adrian and Zotterman, 1926a,b).

nalization by tokens and channels. does an LN layer perform a linear transformation for each token but also squash the extreme values in such a non-linear fashion? understand this, we visualize the points grouped by tokens and channels, respectively. s is plotted in Figure 4 by taking the second and third subplots for ViT from Figure 2, but with a sampled subset of points for more clarity. en we select the channels to plot, we make sure to include the channels with extreme values.

he left two panels of Figure 4, we visualize each token's activations using the same color. observe that all points from any single token do form a straight line. ever, since each token has a different variance, the slopes are different. ens with smaller input x ranges tend to have smaller variance, and the normalization layer will divide their activations using a smaller standard deviation, hence producing a larger slope in the straight line. ectively, they form an S-shaped curve that resembles a tanh function. he two panels on the right, we color each channel's activations using the same color. find that different channels tend to have drastically different input ranges, with only a few channels (e.g., red, green, and pink) exhibiting large extreme values. se are the channels that get squashed the most by the normalization layer.

4 Dynamic Tanh (DyT)

Inspired by the similarity between the shapes of normalization layers and a scaled tanh function, we propose Dynamic Tanh (DyT) as a drop-in replacement for normalization layers. Given an input tensor $\boldsymbol{x}$, a DyT layer is defined as follows:

$$\mathrm{DyT}(\boldsymbol{x}) = \boldsymbol{\gamma} * \tanh(\alpha \boldsymbol{x}) + \boldsymbol{\beta} \tag{2}$$

where α is a learnable scalar parameter that allows scaling the input differently based on its range, accounting for varying x scales (Figure 2). This is also why we name the whole operation "Dynamic" Tanh. $\boldsymbol{\gamma}$ and $\boldsymbol{\beta}$ are learnable, per-channel vector parameters, the same as those used in all normalization layers—they allow the output to scale back to any scales. This is sometimes considered a separate affine layer; for our purposes, we consider them to be part of the DyT layer, just like how normalization layers also include them. See Algorithm 1 for implementation of DyT in Pytorch-like pseudocode.

Algorithm 1 Pseudocode of DyT layer.

```
# input x has the shape of [B, T, C]
# B: batch size, T: tokens, C: dimension

class DyT(Module):
    def __init__(self, C, init_α):
        super().__init__()
        self.α = Parameter(ones(1) * init_α)
        self.γ = Parameter(ones(C))
        self.β = Parameter(zeros(C))

    def forward(self, x):
        x = tanh(self.alpha * x)
        return self.γ * x + self.β
```

Integrating DyT layers into an existing architecture is straightforward: one DyT layer replaces one normalization layer (see Figure 1). This applies to normalization layers within attention blocks, FFN blocks, and the final normalization layer. Although DyT may look like or be considered an activation function, this study only uses it to replace normalization layers without altering any parts of the activation functions in the original architectures, such as GELU or ReLU. Other parts of the networks also remain intact. We also observe that there is little need to tune the hyperparameters used by the original architectures for DyT to perform well.

Initializing parameters. We always simply initialize $\boldsymbol{\gamma}$ to an all-one vector and $\boldsymbol{\beta}$ to an all-zero vector following normalization layers. For the scaler parameter α, a default initialization of 0.5 is generally sufficient, except for LLM training. A detailed analysis of α initialization is provided in Section 7. Unless explicitly stated otherwise, α is initialized to 0.5 in our subsequent experiments.

Remarks. DyT is *not* a new type of normalization layer, as it operates on each input element from a tensor independently during a forward pass without computing statistics or other types of aggregations. It does, however, preserve the effect of normalization layers in squashing the extreme values in a non-linear fashion while almost linearly transforming the very central parts of the input.

5 Experiments

To demonstrate the effectiveness of DyT, we experiment with Transformers and a few other modern architectures across a diverse range of tasks and domains. In each experiment, we replace the LN or RMSNorm in the original architectures with DyT layers and follow the official open-source protocols to train and test both versions of the models. Detailed instructions for reproducing our results are provided in Appendix A. Notably, to highlight the simplicity of adapting DyT, we use hyperparameters identical to those utilized by the normalized counterparts. For completeness, additional experimental results regarding tuning of learning rates and initial values of α are provided in Appendix B.

Supervised learning in vision. We train Vision Transformer (ViT) (Dosovitskiy et al., 2020) and ConvNeXt (Liu et al., 2022) of "Base" and "Large" sizes on the ImageNet-1K classification task (Deng et al., 2009). These models are selected due to their popularity and distinct operations: attention in ViT and convolution in ConvNeXt. Table 1 reports the top-1 classification accuracies. DyT performs slightly better than LN across both architectures and model sizes. We further plot the training loss for ViT-B and ConvNeXt-B in Figure 5. The curves show that the convergence behaviors of DyT and LN-based models are highly aligned.

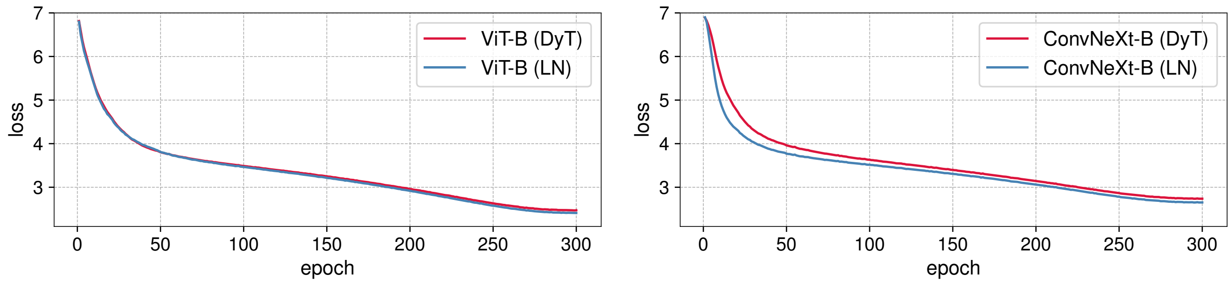

Figure 5 Training loss curves for ViT-B and ConvNeXt-B models. The loss curves for both model types exhibit similar patterns between LN and DyT, suggesting that LN and DyT may share similar learning dynamics.

model	LN	DyT	change
ViT-B	82.3%	82.5%	↑0.2%
ViT-L	83.1%	83.6%	↑0.5%
ConvNeXt-B	83.7%	83.7%	-
ConvNeXt-L	84.3%	84.4%	↑0.1%

Table 1 Supervised classification accuracy on ImageNet-1K. DyT achieves better or similar performance than LN across both architectures and model sizes.

Self-supervised learning in vision. We benchmark with two popular visual self-supervised learning methods: masked autoencoders (MAE) (He et al., 2022) and DINO (Caron et al., 2021). Both by default use Vision Transformers as the backbones, but have different training objectives: MAE is trained with a reconstruction loss, and DINO uses a joint-embedding loss (LeCun, 2022). Following the standard self-supervised learning protocol, we first pretrain models on ImageNet-1K without using any labels and then test the pretrained models by attaching a classification layer and fine-tuning them with labels. The fine-tuning results are presented in Table 2. DyT consistently performs on par with LN in self-supervised learning tasks.

model	LN	DyT	change
MAE ViT-B	83.2%	83.2%	-
MAE ViT-L	85.5%	85.4%	↓0.1%
DINO ViT-B (patch size 16)	83.2%	83.4%	↑0.2%
DINO ViT-B (patch size 8)	84.1%	84.5%	↑0.4%

Table 2 Self-supervised learning accuracy on ImageNet-1K. DyT performs on par with LN across different pretraining methods and model sizes in self-supervised learning tasks.

Diffusion models. We train three Diffusion Transformer (DiT) models (Peebles and Xie, 2023) of sizes B, L and XL on ImageNet-1K (Deng et al., 2009). The patch size is 4, 4, and 2, respectively. Note that in DiT, the LN layers' affine parameters are used for class conditioning in DiT, and we keep them that way in our DyT experiments, only replacing the normalizing transformation with the $\tanh(\alpha \boldsymbol{x})$ function. After training, we evaluate the Fréchet Inception Distance (FID) scores using the standard ImageNet "reference batch", as presented in Table 3. DyT achieves comparable or improved FID over LN.

model	LN	DyT	change
DiT-B	64.9	63.9	↓1.0
DiT-L	45.9	45.7	↓0.2
DiT-XL	19.9	20.8	↑0.9

Table 3 Image generation quality (FID, lower is better) on ImageNet. DyT achieves comparable or superior FID scores to LN across various DiT model sizes.

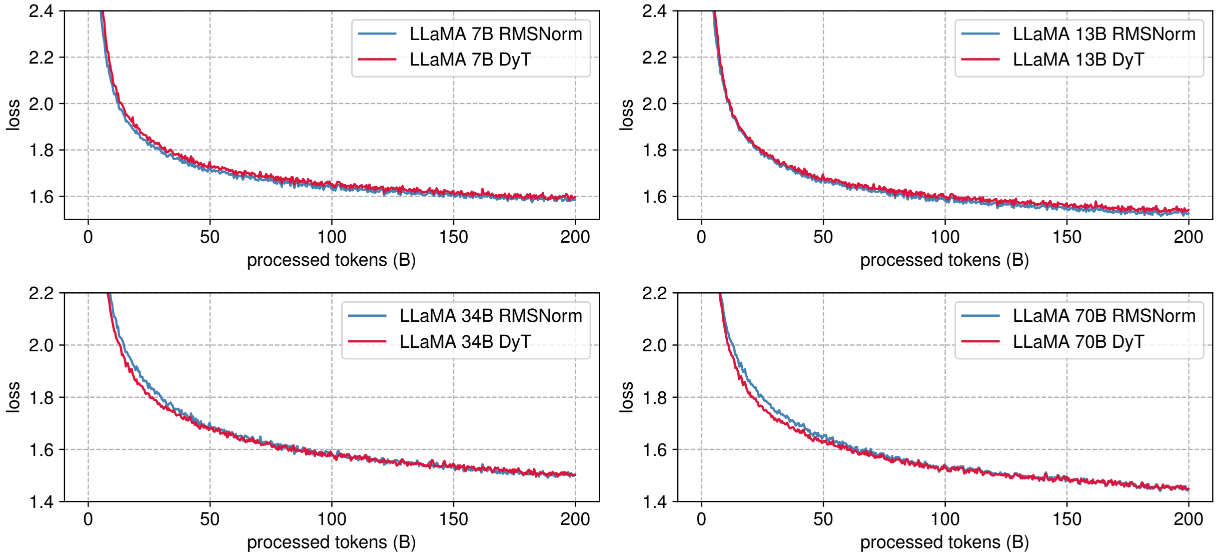

Figure 6 LLaMA pretraining loss. The loss curves of DyT and RMSNorm models are closely aligned across model sizes.

Large Language Models. We pretrain LLaMA 7B, 13B, 34B, and 70B models (Touvron et al., 2023a,b; Dubey et al., 2024) to assess DyT performance relative to RMSNorm (Zhang and Sennrich, 2019), the default normalization layer used in LLaMA. All models are trained on The Pile dataset (Gao et al., 2020) with 200B tokens, following the original recipe outlined in LLaMA (Touvron et al., 2023b). For LLaMA with DyT, we add a learnable scalar parameter after the initial embedding layer, and adjust the initial value of α, as detailed in Section 7. We report the loss value after training and also follow OpenLLaMA (Geng and Liu, 2023) to benchmark the models on 15 zero-shot tasks from `lm-eval` (Gao et al.). As shown in Table 4, DyT performs on par with RMSNorm across all four model sizes. Figure 6 illustrates the loss curves, demonstrating similar trends across all model sizes, with training losses closely aligned throughout training.

score / loss	RMSNorm	DyT	change
LLaMA 7B	0.513 / 1.59	0.513 / 1.60	- / ↑0.01
LLaMA 13B	0.529 / 1.53	0.529 / 1.54	- / ↑0.01
LLaMA 34B	0.536 / 1.50	0.536 / 1.50	- / -
LLaMA 70B	0.549 / 1.45	0.549 / 1.45	- / -

Table 4 Language models' training loss and average performance with 15 zero-shot `lm-eval` tasks. DyT achieves a comparable zero-shot performance and training loss to RMSNorm.

Self-supervised learning in speech. We pretrain two wav2vec 2.0 Transformer models (Baevski et al., 2020) on the LibriSpeech dataset (Panayotov et al., 2015). We report the final validation loss in Table 5. We observe that DyT performs comparably to LN in both model sizes.

model	LN	DyT	change
wav2vec 2.0 Base	1.95	1.95	-
wav2vec 2.0 Large	1.92	1.91	↓0.01

Table 5 Speech pretraining validation loss on LibriSpeech. DyT performs comparably to LN for both wav2vec 2.0 models.

DNA sequence modeling. For the long-range DNA sequence modeling task, we pretrain the HyenaDNA model (Nguyen et al., 2024) and the Caduceus model (Schiff et al., 2024). The pretraining uses the human reference genome data from (GRCh38, 2013), and the evaluation is on GenomicBenchmarks (Grešová et al., 2023). The results are presented in Table 6. DyT maintains performance comparable to LN for this task.

model	LN	DyT	change
HyenaDNA (Nguyen et al., 2024)	85.2%	85.2%	-
Caduceus (Schiff et al., 2024)	86.9%	86.9%	-

Table 6 DNA classification accuracy on GenomicBenchmarks, averaged over each dataset in GenomicBenchmarks. DyT achieves comparable performance to LN.

6 Analysis

We conduct several analyses on important properties of DyT. We begin by evaluating their computational efficiency, followed by two studies examining the roles of the tanh function and the learnable scale α. Finally, we present comparisons with previous methods that aim to remove normalization layers.

6.1 Efficiency of DyT

We benchmark the LLaMA 7B model with RMSNorm or DyT by measuring the total time taken for 100 forward passes (inference) and 100 forward-backward passes (training) using a single sequence of 4096 tokens. Table 7 reports the time required for all RMSNorm or DyT layers and the entire model when running on an Nvidia H100 GPU with BF16 precision. DyT layers significantly reduce computation time compared to RMSNorm layers, with a similar trend observed under FP32 precision. DyT may be a promising choice for efficiency-oriented network design.

	inference		training	
LLaMA 7B	layer	model	layer	model
RMSNorm	2.1s	14.1s	8.3s	42.6s
DyT	1.0s	13.0s	4.8s	39.1s
reduction	↓52.4%	↓7.8%	↓42.2%	↓8.2%

Table 7 Inference and training latency (BF16 precision) for LLaMA 7B with RMSNorm or DyT. DyT achieves a substantial reduction in both inference and training time.

6.2 Ablations of tanh and α

To further investigate the role of tanh and α in DyT, we conduct experiments to evaluate the model's performance when these components are altered or removed.

Replacing and removing tanh. We replace tanh in DyT layers with alternative squashing functions, specifically hardtanh and sigmoid (Figure 7), while keeping the learnable scaler α intact. Furthermore, we assess the impact of completely removing tanh by replacing it with the identity function while still retaining α. As shown in Table 8, the squashing function is essential for stable training. Using the identity function leads to unstable training and divergence, whereas squashing functions enable stable training. Among the squashing functions, tanh performs the best. This is possibly due to its smoothness and zero-centered properties.

model	identity	tanh	hardtanh	sigmoid
ViT-S	58.5% → failed	**80.3%**	79.9%	79.6%
ViT-B	61.0% → failed	**82.5%**	82.2%	81.6%

Table 8 ImageNet-1K classification accuracy with different squashing functions. All experiments follow the same training recipe as the original LN-based models. Squashing functions play a crucial role in preventing divergence, with tanh achieving the highest performance among the three functions. "→ failed" indicates that training diverged after some progress, with the preceding number representing the highest accuracy reached before divergence.

Removing α. Next, we evaluate the impact of removing the learnable α while retaining the squashing functions (tanh, hardtanh, and sigmoid). As shown in Table 9, removing α results in performance degradation across all squashing functions, highlighting the critical role of α in overall model performance.

model	tanh	hardtanh	sigmoid
without α	81.1%	80.7%	80.7%
with α	**82.5%**	**82.2%**	**81.6%**

Table 9 ImageNet-1K classification accuracy with ViT-B. All experiments follow the same training recipe as the original LN-based models. The learnable α is essential for enhancing model performance.

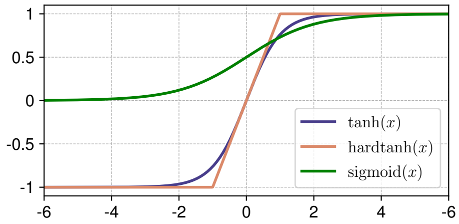

Figure 7 Curves of three squashing functions: tanh, hardtanh, and sigmoid. All three functions squash inputs into a bounded range, but tanh(x) achieves the best performance when used in DyT layers. We suspect it is due to its smoothness and zero-centered properties.

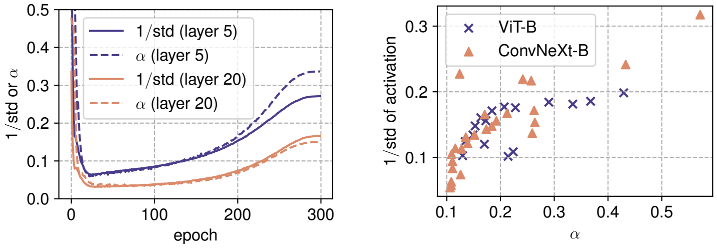

Figure 8 *Left:* For two selected DyT layers from the ViT-B model, we track α and the inverse of the standard deviation (1/std) of activations at the end of each epoch, observing that they evolve together during training. *Right:* We plot the final α values of two trained models, ViT-B and ConvNeXt-B, against the 1/std of the input activations, demonstrating a strong correlation between the two values.

6.3 Values of α

During training. Our analysis reveals that the α closely tracks the 1/std of activations throughout training. As illustrated in the left panel of Figure 8, α first decrease and then increase during training, but always fluctuate consistently with the standard deviation of input activations. This supports the important role of α in maintaining activations within a suitable range, which leads to stable and effective training.

After training. Our further analysis of the final values of α in trained networks reveals a strong correlation with the 1/std of the input activations. As shown on the right panel of Figure 8, higher 1/std values generally correspond to larger α values, and vice versa. Additionally, we observe that deeper layers tend to have activations with larger standard deviations. This trend aligns with characteristics of deep residual networks, as shown in Brock et al. (2021a) for ConvNets, and Sun et al. (2025) for Transformers.

Both analyses suggest that α functions partially as a normalization mechanism by learning values approximating 1/std of the input activations. Unlike LN, which normalizes the activations per token, α normalizes the entire input activations collectively. Consequently, α alone cannot suppress extreme values in a non-linear fashion.

6.4 Comparison with Other Methods

To further assess DyT's effectiveness, we compare it with other methods that also enable training Transformers without normalization layers. These methods can be broadly categorized into initialization-based and weight-normalization-based methods. We consider two popular initialization-based methods, Fixup (Zhang et al., 2019; Huang et al., 2020) and SkipInit (De and Smith, 2020; Bachlechner et al., 2021). Both methods aim to mitigate training instabilities by adjusting the initial parameter values to prevent large gradients and activations at the start of training, thereby enabling stable learning without normalization layers. In contrast, weight-normalization-based methods impose constraints on network weights throughout training to maintain stable learning dynamics in the absence of normalization layers. We include one such method, σReparam (Zhai et al., 2023), which controls the spectral norm of the weights to promote stable learning.

model	LN	Fixup	SkipInit	σReparam	DyT
ViT-B	82.3%	77.2%	74.1%	82.5%	**82.8%**
ViT-L	83.1%	78.1%	75.6%	83.0%	**83.6%**
MAE ViT-B	83.2%	73.7%	73.1%	83.2%	**83.7%**
MAE ViT-L	85.5%	74.1%	74.0%	85.4%	**85.8%**

Table 10 Classification accuracy on ImageNet-1K. DyT consistently achieves superior performance over other methods.

Table 10 summarizes the results of two ViT-based tasks. We closely follow the original protocols outlined in their respective papers. However, we find that both initialization-based methods, Fixup and SkipInit, require significantly lower learning rates to prevent training divergence. To ensure a fair comparison, we conduct a simple learning rate search for all methods, including DyT. This produces results that differ from those reported in Section 5, where no hyperparameter is tuned. Overall, the results show that DyT consistently outperforms all other tested methods across different configurations.

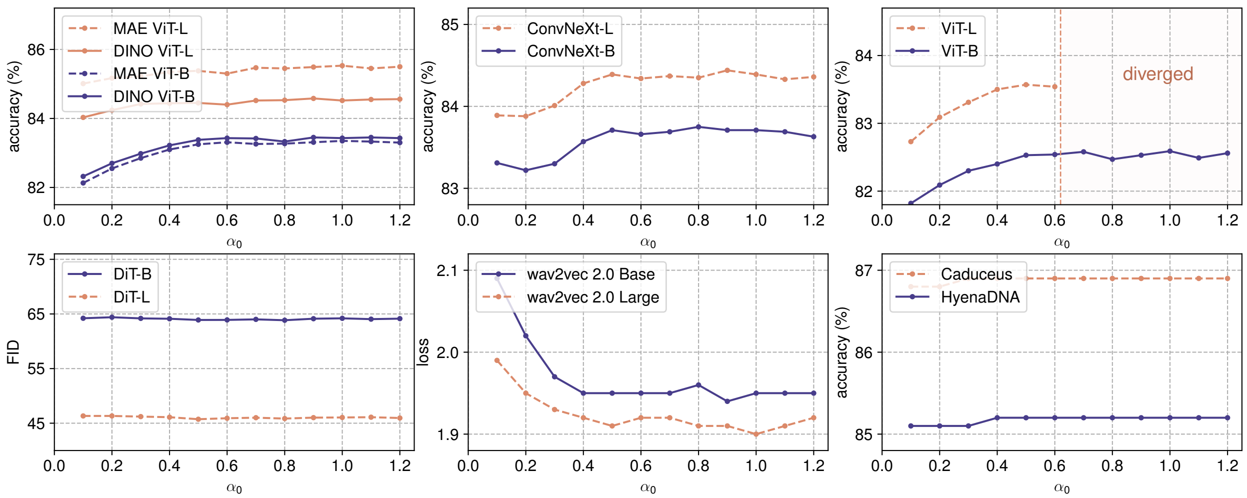

Figure 9 Performance of different tasks across different α_0 values. We benchmark the performance of all non-LLM tasks used in Section 5 with different initial values of α. Performance remains stable across a wide range of α_0 values. The only exception is that supervised ViT-L models (top right panel) will diverge for α_0 values larger than 0.6.

7 Initialization of α

We find that tuning the initialization of α (denoted α_0) rarely leads to significant performance improvements. The only exception is LLM training, where careful tuning of α_0 yields noticeable performance gains. In this section, we detail our findings on the impact of α initialization.

7.1 Initialization of α for Non-LLM Models

Non-LLM models are relatively insensitive to α_0. Figure 9 shows the effect of varying α_0 on validation performance across different tasks. All experiments follow the original setup and hyperparameters of their respective recipe. We observe that performance remains stable across a wide range of α_0 values, with values between 0.5 and 1.2 generally yielding good results. We observe that adjusting α_0 typically affects only the early stages of the training curves. The main exception is supervised ViT-L experiments, where training becomes unstable and diverges when α_0 exceeds 0.6. In such cases, reducing the learning rate restores stability, as detailed below.

Smaller α_0 results in more stable training. Building on previous observations, we further analyze the factors contributing to training instability. Our findings suggest that increasing either the model size or the learning rate requires lowering α_0 to ensure stable training. Conversely, a higher α_0 requires a lower learning rate to mitigate training instability. Figure 10 shows the ablation of the training stability of supervised ViT with ImageNet-1K dataset. We vary learning rates, model sizes, and α_0 values. Training a larger model is more prone to failure, requiring smaller α_0 values or learning rates for stable training. A similar instability pattern

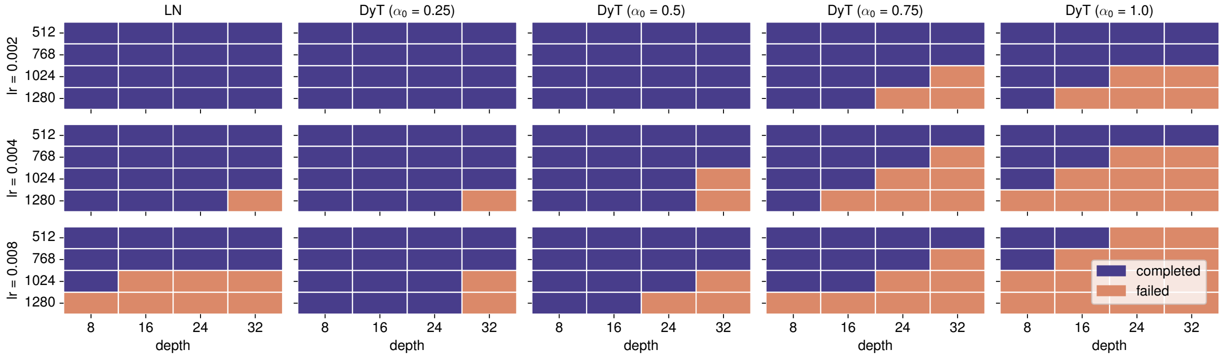

Figure 10 Stability across varying α_0 values, learning rates, and model sizes. We train supervised ViT models on the ImageNet-1K dataset and observe that larger models are more prone to instability for both LN and DyT models. Lowering the learning rate or reducing α_0 enhances stability. LN shows similar stability to DyT with $\alpha_0 = 0.5$.

is also observed in LN-based models under comparable conditions, and setting $\alpha_0 = 0.5$ results in a stability pattern similar to that of LN.

Setting $\alpha_0 = 0.5$ as the default. Based on our findings, we set $\alpha_0 = 0.5$ as the default value for all non-LLM models. This setting provides training stability comparable to LN while maintaining strong performance.

7.2 Initialization of α for LLMs

Tuning α_0 enhances LLM performance. As discussed earlier, the default setting of $\alpha_0 = 0.5$ generally performs well across most tasks. However, we find tuning α_0 can substantially improve LLM performance. We tune α_0 across LLaMA models by pretraining each on 30B tokens and comparing their training losses. Table 11 summarizes the tuned α_0 values for each model. Two key findings emerge:

1. **Larger models require smaller α_0 values.** Once the optimal α_0 is determined for smaller models, the search space for larger models can be reduced accordingly.
2. **Higher α_0 values for attention blocks improve performance.** We find that initializing α with higher values for DyT layers in attention blocks and lower values for DyT layers in other locations (i.e., within FFN blocks or before the final linear projection) improves performance.

model	width	depth	optimal α_0 (attention/other)
LLaMA 7B	4096	32	0.8/0.2
LLaMA 13B	5120	40	0.6/0.15
LLaMA 34B	8196	48	0.2/0.05
LLaMA 70B	8196	80	0.2/0.05

Table 11 Optimal α_0 for different LLaMA models. Larger models require smaller α_0 values. We find it is important to initialize α differently in (1) attention blocks ("attention"), versus (2) the FFN blocks, and the final DyT layer before outputs ("other"). α_0 in attention blocks require larger values.

To further illustrate the impact of α_0 tuning, Figure 11 presents heatmaps of loss values of two LLaMA models. Both models benefit from higher α_0 in attention blocks, leading to reduced training loss.

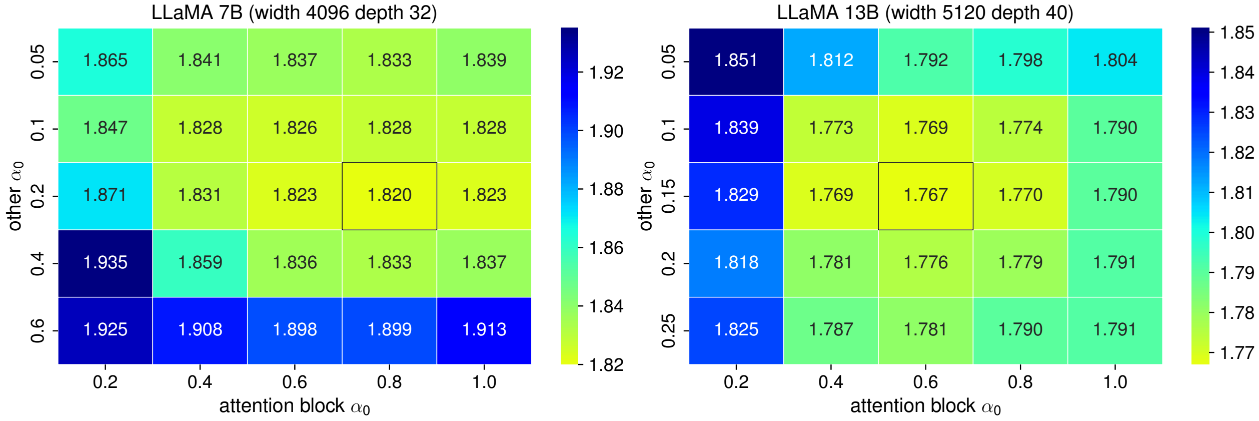

Figure 11 Heatmaps of loss values at 30B tokens for different α_0 settings. Both LLaMA models benefit from increased α_0 in attention blocks.

Model width primarily determines α_0 selection. We also investigate the influence of model width and depth on the optimal α_0. We find that the model width is critical in determining the optimal α_0, while model depth has minimal influence. Table 12 shows the optimal α_0 values across different widths and depths, showing that wider networks benefit from smaller α_0 values for optimal performance. On the other hand, model depth has negligible impact on the choice of α_0.

width / depth	8	16	32	64
1024	1.0/1.0	1.0/1.0	1.0/1.0	1.0/1.0
2048	1.0/0.5	1.0/0.5	1.0/0.5	1.0/0.5
4096	0.8/0.2	0.8/0.2	0.8/0.2	0.8/0.2
8192	0.2/0.05	0.2/0.05	0.2/0.05	0.2/0.05

Table 12 Optimal α_0 (attention / other) across model widths and depths in LLaMA training. Model width significantly impacts the choice of α_0, with wider networks requiring smaller values. In contrast, model depth has negligible influence.

As can be seen in Table 12, the wider the network, the more uneven initialization for "attention" and "other" is needed. We hypothesize that the sensitivity of LLM's α initialization is related to their excessively large widths compared to other models.

8 Related Work

Mechanisms of Normalization layers. There has been a rich line of work investigating normalization layers' role in enhancing model performance through various mechanisms. These include stabilizing gradient flow during training (Balduzzi et al., 2017; Daneshmand et al., 2020; Lubana et al., 2021), reducing sensitivity to weight initialization (Zhang et al., 2019; De and Smith, 2020; Shao et al., 2020), moderating outlier eigenvalues (Bjorck et al., 2018; Karakida et al., 2019), auto-tuning learning rates (Arora et al., 2018; Tanaka and Kunin, 2021), and smoothing the loss landscape for more stable optimization (Santurkar et al., 2018). These earlier works focused on studying batch normalization. Recent studies (Lyu et al., 2022; Dai et al., 2024; Mueller et al., 2024) further highlight the connection between normalization layers and sharpness reduction, which contributes to better generalization.

Normalization in Transformers. With the rise of Transformer (Vaswani et al., 2017), research has increasingly focused on layer normalization (Ba et al., 2016), which has proven particularly effective for sequential data in natural language tasks (Nguyen and Salazar, 2019; Xu et al., 2019; Xiong et al., 2020). Recent work (Ni et al., 2024) reveals that layer normalization introduces strong non-linearity, enhancing the model's representational capacity. Additionally, studies (Loshchilov et al., 2024; Li et al., 2024) demonstrate that modifying the location of normalization layers within Transformers can improve convergence properties.

Removing normalization. Many studies have explored how to train deep models without normalization layers. Several works (Zhang et al., 2019; De and Smith, 2020; Bachlechner et al., 2021) explore alternative weight initialization schemes to stabilize training. The pioneering work by Brock et al. (2021a,b) show that high-performing ResNets can be trained without normalization (Smith et al., 2023) through combination of initialization techniques (De and Smith, 2020), weight normalization (Salimans and Kingma, 2016; Huang et al., 2017; Qiao et al., 2019), and adaptive gradient clipping (Brock et al., 2021b). Additionally, their training strategy incorporates extensive data augmentation (Cubuk et al., 2020) and regularization (Srivastava et al., 2014; Huang et al., 2016). The studies above are based on various ConvNet models.

In Transformer architectures, He and Hofmann (2023) explore modifications to Transformer blocks that reduce reliance on normalization layers and skip connections. Alternatively, Heimersheim (2024) propose a method to gradually remove LN from pretrained networks by fine-tuning the model after removing each normalization layer. Unlike previous approaches, DyT requires minimal modifications to both the architecture and the training recipe. Despite its simplicity, DyT achieves stable training and comparable performance.

9 Limitations

We conduct experiments on networks using either LN or RMSNorm because of their popularity in Transformers and other modern architectures. Preliminary experiments (see Appendix C) indicate that DyT struggles to replace BN directly in classic networks like ResNets. It remains to be studied in more depth whether and how DyT can adapt to models with other types of normalization layers.

10 Conclusion

In this work, we demonstrate modern neural networks, in particular Transformers, can be trained without normalization layers. This is done through Dynamic Tanh (DyT), a simple replacement for traditional normalization layers. It adjusts the input activation range via a learnable scaling factor α and then squashes the extreme values through an S-shaped tanh function. Although a simpler function, it effectively captures the behavior of normalization layers. Under various settings, models with DyT match or exceed the performance of their normalized counterparts. These findings challenge the conventional understanding of the necessity of normalization layers in training modern neural networks. Our study also contributes to understanding the mechanisms of normalization layers, one of the most fundamental building blocks in deep neural networks.

References

Edgar D Adrian. The impulses produced by sensory nerve endings: Part 1. *The Journal of Physiology*, 1926.

Edgar D Adrian and Yngve Zotterman. The impulses produced by sensory nerve-endings: Part 2. the response of a single end-organ. *The Journal of Physiology*, 1926a.

Edgar D Adrian and Yngve Zotterman. The impulses produced by sensory nerve endings: Part 3. impulses set up by touch and pressure. *The Journal of Physiology*, 1926b.

Sanjeev Arora, Zhiyuan Li, and Kaifeng Lyu. Theoretical analysis of auto rate-tuning by batch normalization. *arXiv preprint arXiv:1812.03981*, 2018.

Jimmy Lei Ba, Jamie Ryan Kiros, and Geoffrey E Hinton. Layer normalization. *arXiv preprint arXiv:1607.06450*, 2016.

Thomas Bachlechner, Bodhisattwa Prasad Majumder, Henry Mao, Gary Cottrell, and Julian McAuley. Rezero is all you need: Fast convergence at large depth. In *UAI*, 2021.

Alexei Baevski, Yuhao Zhou, Abdelrahman Mohamed, and Michael Auli. wav2vec 2.0: A framework for self-supervised learning of speech representations. *NeurIPS*, 2020.

Jinze Bai, Shuai Bai, Yunfei Chu, Zeyu Cui, Kai Dang, Xiaodong Deng, Yang Fan, Wenbin Ge, Yu Han, Fei Huang, et al. Qwen technical report. *arXiv preprint arXiv:2309.16609*, 2023.

David Balduzzi, Marcus Frean, Lennox Leary, JP Lewis, Kurt Wan-Duo Ma, and Brian McWilliams. The shattered gradients problem: If resnets are the answer, then what is the question? In *ICML*, 2017.

Nils Bjorck, Carla P Gomes, Bart Selman, and Kilian Q Weinberger. Understanding batch normalization. *NeurIPS*, 2018.

Andrew Brock, Soham De, and Samuel L Smith. Characterizing signal propagation to close the performance gap in unnormalized resnets. *arXiv preprint arXiv:2101.08692*, 2021a.

Andrew Brock, Soham De, Samuel L Smith, and Karen Simonyan. High-performance large-scale image recognition without normalization. In *ICML*, 2021b.

Zheng Cai, Maosong Cao, Haojiong Chen, Kai Chen, Keyu Chen, Xin Chen, Xun Chen, Zehui Chen, Zhi Chen, Pei Chu, et al. Internlm2 technical report. *arXiv preprint arXiv:2403.17297*, 2024.

Mathilde Caron, Hugo Touvron, Ishan Misra, Hervé Jégou, Julien Mairal, Piotr Bojanowski, and Armand Joulin. Emerging properties in self-supervised vision transformers. In *ICCV*, 2021.

Ekin D Cubuk, Barret Zoph, Jonathon Shlens, and Quoc V Le. Randaugment: Practical automated data augmentation with a reduced search space. In *CVPR Workshops*, 2020.

Yan Dai, Kwangjun Ahn, and Suvrit Sra. The crucial role of normalization in sharpness-aware minimization. *NeurIPS*, 2024.

Hadi Daneshmand, Jonas Kohler, Francis Bach, Thomas Hofmann, and Aurelien Lucchi. Batch normalization provably avoids ranks collapse for randomly initialised deep networks. *NeurIPS*, 2020.

Soham De and Sam Smith. Batch normalization biases residual blocks towards the identity function in deep networks. *NeurIPS*, 2020.

Jia Deng, Wei Dong, Richard Socher, Li-Jia Li, Kai Li, and Li Fei-Fei. Imagenet: A large-scale hierarchical image database. In *CVPR*, 2009.

Alexey Dosovitskiy, Lucas Beyer, Alexander Kolesnikov, Dirk Weissenborn, Xiaohua Zhai, Thomas Unterthiner, Mostafa Dehghani, Matthias Minderer, Georg Heigold, Sylvain Gelly, et al. An image is worth 16x16 words: Transformers for image recognition at scale. *arXiv preprint arXiv:2010.11929*, 2020.

Abhimanyu Dubey, Abhinav Jauhri, Abhinav Pandey, Abhishek Kadian, Ahmad Al-Dahle, Aiesha Letman, Akhil Mathur, Alan Schelten, Amy Yang, Angela Fan, et al. The llama 3 herd of models. *arXiv preprint arXiv:2407.21783*, 2024.

Leo Feng, Frederick Tung, Mohamed Osama Ahmed, Yoshua Bengio, and Hossein Hajimirsadegh. Were rnns all we needed? *arXiv preprint arXiv:2410.01201*, 2024.

Foundation Model Stack. Github: FMS FSDP. https://github.com/foundation-model-stack/fms-fsdp. Accessed: 2025-01-23.

Leo Gao, Jonathan Tow, Baber Abbasi, Stella Biderman, Sid Black, Anthony DiPofi, Charles Foster, Laurence Golding, Jeffrey Hsu, Alain Le Noac'h, Haonan Li, Kyle McDonell, Niklas Muennighoff, Chris Ociepa, Jason Phang, Laria Reynolds, Hailey Schoelkopf, Aviya Skowron, Lintang Sutawika, Eric Tang, Anish Thite, Ben Wang, Kevin Wang, and Andy Zou. A framework for few-shot language model evaluation. https://zenodo.org/records/10256836.

Leo Gao, Stella Biderman, Sid Black, Laurence Golding, Travis Hoppe, Charles Foster, Jason Phang, Horace He, Anish Thite, Noa Nabeshima, Shawn Presser, and Connor Leahy. The Pile: An 800gb dataset of diverse text for language modeling. *arXiv preprint arXiv:2101.00027*, 2020.

Xinyang Geng and Hao Liu. Openllama: An open reproduction of llama, 2023. https://github.com/openlm-research/open_llama.

Ensembl GRCh38. p13 (genome reference consortium human build 38), insdc assembly, 2013.

Katarína Grešová, Vlastimil Martinek, David Čechák, Petr Šimeček, and Panagiotis Alexiou. Genomic benchmarks: a collection of datasets for genomic sequence classification. *BMC Genomic Data*, 2023.

Albert Gu and Tri Dao. Mamba: Linear-time sequence modeling with selective state spaces. *arXiv preprint arXiv:2312.00752*, 2023.

Daya Guo, Dejian Yang, Haowei Zhang, Junxiao Song, Ruoyu Zhang, Runxin Xu, Qihao Zhu, Shirong Ma, Peiyi Wang, Xiao Bi, et al. Deepseek-r1: Incentivizing reasoning capability in llms via reinforcement learning. *arXiv preprint arXiv:2501.12948*, 2025.

HazyResearch. Github: Hyenadna. https://github.com/HazyResearch/hyena-dna.git. Accessed: 2025-01-23.

Bobby He and Thomas Hofmann. Simplifying transformer blocks. *arXiv preprint arXiv:2311.01906*, 2023.

Kaiming He, Xiangyu Zhang, Shaoqing Ren, and Jian Sun. Deep residual learning for image recognition. In *CVPR*, 2016.

Kaiming He, Xinlei Chen, Saining Xie, Yanghao Li, Piotr Dollár, and Ross Girshick. Masked autoencoders are scalable vision learners. In *CVPR*, 2022.

Stefan Heimersheim. You can remove gpt2's layernorm by fine-tuning. *arXiv preprint arXiv:2409.13710*, 2024.

Gao Huang, Yu Sun, Zhuang Liu, Daniel Sedra, and Kilian Q Weinberger. Deep networks with stochastic depth. In *ECCV*, 2016.

Lei Huang, Xianglong Liu, Yang Liu, Bo Lang, and Dacheng Tao. Centered weight normalization in accelerating training of deep neural networks. In *ICCV*, 2017.

Lei Huang, Jie Qin, Yi Zhou, Fan Zhu, Li Liu, and Ling Shao. Normalization techniques in training dnns: Methodology, analysis and application. *TPAMI*, 2023.

Xiao Shi Huang, Felipe Perez, Jimmy Ba, and Maksims Volkovs. Improving transformer optimization through better initialization. In *ICML*, 2020.

Sergey Ioffe and Christian Szegedy. Batch normalization: Accelerating deep network training by reducing internal covariate shift. In *ICML*, 2015.

Albert Q Jiang, Alexandre Sablayrolles, Arthur Mensch, Chris Bamford, Devendra Singh Chaplot, Diego de las Casas, Florian Bressand, Gianna Lengyel, Guillaume Lample, Lucile Saulnier, et al. Mistral 7b. *arXiv preprint arXiv:2310.06825*, 2023.

Ryo Karakida, Shotaro Akaho, and Shun-ichi Amari. The normalization method for alleviating pathological sharpness in wide neural networks. *NeurIPS*, 2019.

Kuleshov Group. Github: Caduceus. https://github.com/kuleshov-group/caduceus.git. Accessed: 2025-01-23.

Yann LeCun. A path towards autonomous machine intelligence version 0.9.2, 2022-06-27. *Open Review*, 2022.

Pengxiang Li, Lu Yin, and Shiwei Liu. Mix-ln: Unleashing the power of deeper layers by combining pre-ln and post-ln. *arXiv preprint arXiv:2412.13795*, 2024.

Aixin Liu, Bei Feng, Bin Wang, Bingxuan Wang, Bo Liu, Chenggang Zhao, Chengqi Dengr, Chong Ruan, Damai Dai, Daya Guo, et al. Deepseek-v2: A strong, economical, and efficient mixture-of-experts language model. *arXiv preprint arXiv:2405.04434*, 2024.

Zhuang Liu, Hanzi Mao, Chao-Yuan Wu, Christoph Feichtenhofer, Trevor Darrell, and Saining Xie. A convnet for the 2020s. In *CVPR*, 2022.

Ilya Loshchilov, Cheng-Ping Hsieh, Simeng Sun, and Boris Ginsburg. ngpt: Normalized transformer with representation learning on the hypersphere. *arXiv preprint arXiv:2410.01131*, 2024.

Ekdeep S Lubana, Robert Dick, and Hidenori Tanaka. Beyond batchnorm: Towards a unified understanding of normalization in deep learning. *NeurIPS*, 2021.

Kaifeng Lyu, Zhiyuan Li, and Sanjeev Arora. Understanding the generalization benefit of normalization layers: Sharpness reduction. *NeurIPS*, 2022.

Meta Research. Github: ConvNeXt. https://github.com/facebookresearch/ConvNeXt, a. Accessed: 2025-01-23.

Meta Research. Github: DINO. https://github.com/facebookresearch/dino, b. Accessed: 2025-01-23.

Meta Research. Github: DiT. https://github.com/facebookresearch/DiT, c. Accessed: 2025-01-23.

Meta Research. Github: MAE. https://github.com/facebookresearch/mae, d. Accessed: 2025-01-23.

Meta Research. Github: wav2vec 2.0. https://github.com/facebookresearch/fairseq, e. Accessed: 2025-01-23.

Maximilian Mueller, Tiffany Vlaar, David Rolnick, and Matthias Hein. Normalization layers are all that sharpness-aware minimization needs. *NeurIPS*, 2024.

Eric Nguyen, Michael Poli, Marjan Faizi, Armin Thomas, Michael Wornow, Callum Birch-Sykes, Stefano Massaroli, Aman Patel, Clayton Rabideau, Yoshua Bengio, et al. Hyenadna: Long-range genomic sequence modeling at single nucleotide resolution. *NeurIPS*, 2024.

Toan Q Nguyen and Julian Salazar. Transformers without tears: Improving the normalization of self-attention. *arXiv preprint arXiv:1910.05895*, 2019.

Yunhao Ni, Yuxin Guo, Junlong Jia, and Lei Huang. On the nonlinearity of layer normalization. *arXiv preprint arXiv:2406.01255*, 2024.

Vassil Panayotov, Guoguo Chen, Daniel Povey, and Sanjeev Khudanpur. Librispeech: an asr corpus based on public domain audio books. In *ICASSP*, 2015.

William Peebles and Saining Xie. Scalable diffusion models with transformers. In *ICCV*, 2023.

Siyuan Qiao, Huiyu Wang, Chenxi Liu, Wei Shen, and Alan Yuille. Micro-batch training with batch-channel normalization and weight standardization. *arXiv preprint arXiv:1903.10520*, 2019.

Colin Raffel, Noam Shazeer, Adam Roberts, Katherine Lee, Sharan Narang, Michael Matena, Yanqi Zhou, Wei Li, and Peter J Liu. Exploring the limits of transfer learning with a unified text-to-text transformer. *JMLR*, 2020.

Tim Salimans and Durk P Kingma. Weight normalization: A simple reparameterization to accelerate training of deep neural networks. *NeurIPS*, 2016.

Shibani Santurkar, Dimitris Tsipras, Andrew Ilyas, and Aleksander Madry. How does batch normalization help optimization? *NeurIPS*, 2018.

Yair Schiff, Chia-Hsiang Kao, Aaron Gokaslan, Tri Dao, Albert Gu, and Volodymyr Kuleshov. Caduceus: Bi-directional equivariant long-range dna sequence modeling. *arXiv preprint arXiv:2403.03234*, 2024.

Jie Shao, Kai Hu, Changhu Wang, Xiangyang Xue, and Bhiksha Raj. Is normalization indispensable for training deep neural network? *NeurIPS*, 2020.

Karen Simonyan and Andrew Zisserman. Very deep convolutional networks for large-scale image recognition. *arXiv preprint arXiv:1409.1556*, 2014.

Samuel L Smith, Andrew Brock, Leonard Berrada, and Soham De. Convnets match vision transformers at scale. *arXiv preprint arXiv:2310.16764*, 2023.

Nitish Srivastava, Geoffrey Hinton, Alex Krizhevsky, Ilya Sutskever, and Ruslan Salakhutdinov. Dropout: a simple way to prevent neural networks from overfitting. *JMLR*, 2014.

Wenfang Sun, Xinyuan Song, Pengxiang Li, Lu Yin, Yefeng Zheng, and Shiwei Liu. The curse of depth in large language models. *arXiv preprint arXiv:2502.05795*, 2025.

Yu Sun, Xinhao Li, Karan Dalal, Jiarui Xu, Arjun Vikram, Genghan Zhang, Yann Dubois, Xinlei Chen, Xiaolong Wang, Sanmi Koyejo, et al. Learning to (learn at test time): Rnns with expressive hidden states. *arXiv preprint arXiv:2407.04620*, 2024.

Christian Szegedy, Vincent Vanhoucke, Sergey Ioffe, Jon Shlens, and Zbigniew Wojna. Rethinking the inception architecture for computer vision. In *CVPR*, 2016.

Hidenori Tanaka and Daniel Kunin. Noether's learning dynamics: Role of symmetry breaking in neural networks. *NeurIPS*, 2021.

Ilya O Tolstikhin, Neil Houlsby, Alexander Kolesnikov, Lucas Beyer, Xiaohua Zhai, Thomas Unterthiner, Jessica Yung, Andreas Steiner, Daniel Keysers, Jakob Uszkoreit, et al. Mlp-mixer: An all-mlp architecture for vision. *NeurIPS*, 2021.

Hugo Touvron, Thibaut Lavril, Gautier Izacard, Xavier Martinet, Marie-Anne Lachaux, Timothée Lacroix, Baptiste Rozière, Naman Goyal, Eric Hambro, Faisal Azhar, et al. Llama: Open and efficient foundation language models. *arXiv preprint arXiv:2302.13971*, 2023a.

Hugo Touvron, Louis Martin, Kevin Stone, Peter Albert, Amjad Almahairi, Yasmine Babaei, Nikolay Bashlykov, Soumya Batra, Prajjwal Bhargava, Shruti Bhosale, et al. Llama 2: Open foundation and fine-tuned chat models. *arXiv preprint arXiv:2307.09288*, 2023b.

Dmitry Ulyanov, Andrea Vedaldi, and Victor Lempitsky. Instance normalization: The missing ingredient for fast stylization. *arXiv preprint arXiv:1607.08022*, 2016.

Ashish Vaswani, Noam Shazeer, Niki Parmar, Jakob Uszkoreit, Llion Jones, Aidan N Gomez, Łukasz Kaiser, and Illia Polosukhin. Attention is all you need. *NeurIPS*, 2017.

Yuxin Wu and Kaiming He. Group normalization. In *ECCV*, 2018.

Saining Xie, Ross Girshick, Piotr Dollár, Zhuowen Tu, and Kaiming He. Aggregated residual transformations for deep neural networks. In *CVPR*, 2017.

Ruibin Xiong, Yunchang Yang, Di He, Kai Zheng, Shuxin Zheng, Chen Xing, Huishuai Zhang, Yanyan Lan, Liwei Wang, and Tieyan Liu. On layer normalization in the transformer architecture. In *ICML*, 2020.

Jingjing Xu, Xu Sun, Zhiyuan Zhang, Guangxiang Zhao, and Junyang Lin. Understanding and improving layer normalization. *NeurIPS*, 2019.

An Yang, Baosong Yang, Binyuan Hui, Bo Zheng, Bowen Yu, Chang Zhou, Chengpeng Li, Chengyuan Li, Dayiheng Liu, Fei Huang, et al. Qwen2 technical report. *arXiv preprint arXiv:2407.10671*, 2024.

Shuangfei Zhai, Tatiana Likhomanenko, Etai Littwin, Dan Busbridge, Jason Ramapuram, Yizhe Zhang, Jiatao Gu, and Joshua M Susskind. Stabilizing transformer training by preventing attention entropy collapse. In *ICML*, 2023.

Biao Zhang and Rico Sennrich. Root mean square layer normalization. *NeurIPS*, 2019.

Hongyi Zhang, Yann N Dauphin, and Tengyu Ma. Fixup initialization: Residual learning without normalization. *arXiv preprint arXiv:1901.09321*, 2019.

Pan Zhang, Xiaoyi Dong, Yuhang Zang, Yuhang Cao, Rui Qian, Lin Chen, Qipeng Guo, Haodong Duan, Bin Wang, Linke Ouyang, et al. Internlm-xcomposer-2.5: A versatile large vision language model supporting long-contextual input and output. *arXiv preprint arXiv:2407.03320*, 2024.

Appendix

A Experimental Settings

Supervised image classification. For all supervised classification experiments on ImageNet-1K, we follow the training recipes from ConvNeXt (Meta Research, a). For ConvNeXt-B and ConvNeXt-L, we use the original hyperparameters without modification. ViT-B and ViT-L models use the same hyperparameters as ConvNeXt-B, except that for ViT-L, the beta parameters for AdamW are set to (0.9, 0.95), and the stochastic depth rates are set to 0.1 for ViT-B and 0.4 for ViT-L.

Diffusion models. We use the official implementation (Meta Research, c) for training all DiT models. We find that the default learning rate is suboptimal for the models considered in this paper. To address this, we conduct a simple learning rate search with the LN models and apply the tuned learning rates directly to the DyT models. We also observe that the zero initialization negatively affects the performance of DyT models. Therefore, we retain the zero initialization for LN models but remove the zero initialization for DyT models.

Large Language Models. In our implementation of LLaMA models (Touvron et al., 2023a,b; Dubey et al., 2024) with DyT, we introduce an additional learnable scalar parameter immediately after the embedding layer, before any Transformer blocks. We initialize it to the square root of the model embedding dimension $\sqrt{d}$. Without this scaling scalar, we find that the magnitudes of model activations at the beginning of training are too small, and the training struggles to progress. The issue is mitigated by incorporating a learnable scalar, and the model can converge normally. This addition of a scalar is similar to the original Transformer (Vaswani et al., 2017) design, which uses a fixed scalar of the same value at the same position.

We train all our LLaMA models on the Pile dataset (Gao et al., 2020). We use the codebase from `FMS-FSDP` (Foundation Model Stack), which provides a default training recipe for the 7B model that closely follows the LLaMA 2 paper (Touvron et al., 2023b). We maintain the learning rate at the default 3e-4 for 7B and 13B and 1.5e-4 for 34B and 70B, in line with LLaMA 2. The batch size is set to 4M tokens and each model is trained on a total of 200B tokens.

For evaluation, we test the pretrained models on 15 zero-shot commonsense reasoning tasks from `lm-eval` (Gao et al.): `anli_r1`, `anli_r2`, `anli_r3`, `arc_challenge`, `arc_easy`, `boolq`, `hellaswag`, `openbookqa`, `piqa`, `record`, `rte`, `truthfulqa_mc1`, `truthfulqa_mc2`, `wic`, and `winogrande`. The selection closely follows that of OpenLLaMA (Geng and Liu, 2023). We report the average performance across all tasks.

Self-supervised learning in speech. For both wav2vec 2.0 models, we retain the first group normalization layer from the original architecture, as it functions primarily as data normalization to handle the unnormalized input data. We use the official implementation (Meta Research, e) without modifying hyperparameters for both the Base and Large models. We report the final validation loss.

Other tasks. For all other tasks, MAE (He et al., 2022), DINO (Caron et al., 2021), HyenaDNA (Nguyen et al., 2024) and Caduceus (Schiff et al., 2024), we directly use the publicly released code (Meta Research, d,b; HazyResearch; Kuleshov Group), without hyperparameter tuning, for both models with LN and DyT.

B Hyperparameters

We present additional experiments to evaluate the impact of hyperparameter tuning, specifically focusing on the learning rate and initialization of α for all non-LLM models.

Tuning learning rate. Table 13 summarizes performance comparisons between models trained with original versus tuned learning rates. Results indicate that tuning the learning rate provides only modest performance improvements for DyT models. This suggests that the original hyperparameters, initially optimized for LN models, are already well-suited for DyT models. This observation underscores the inherent similarity between the DyT and LN models.

model	LN (original)	DyT (original)	LN (tuned)	DyT (tuned)
ViT-B	82.3% (4e-3)	82.5% (4e-3)	-	82.8% (6e-3)
ViT-L	83.1% (4e-3)	83.6% (4e-3)	-	-
ConvNeXt-B	83.7% (4e-3)	83.7% (4e-3)	-	-
ConvNeXt-L	84.3% (4e-3)	84.4% (4e-3)	-	-
MAE ViT-B	83.2% (2.4e-3)	83.2% (2.4e-3)	-	83.7% (3.2e-3)
MAE ViT-L	85.5% (2.4e-3)	85.4% (2.4e-3)	-	85.8% (3.2e-3)
DINO ViT-B (patch size 16)	83.2% (7.5e-4)	83.4% (7.5e-4)	83.3% (1e-3)	-
DINO ViT-B (patch size 8)	84.1% (5e-4)	84.5% (5e-4)	-	-
DiT-B	64.9 (4e-4)	63.9 (4e-4)	-	-
DiT-L	45.9 (4e-4)	45.7 (4e-4)	-	-
DiT-XL	19.9 (4e-4)	20.8 (4e-4)	-	-
wav2vec 2.0 Base	1.95 (5e-4)	1.95 (5e-4)	-	1.94 (6e-4)
wav2vec 2.0 Large	1.92 (3e-4)	1.91 (3e-4)	-	-
HyenaDNA	85.2% (6e-4)	85.2% (6e-4)	-	-
Caduceus	86.9% (8e-3)	86.9% (8e-3)	-	-

Table 13 Performance comparison between original and tuned learning rates for LN and DyT models. Results show that tuning learning rates provide only modest performance improvements for DyT models, suggesting that the default hyperparameters optimized for LN models are already well-suited for DyT models. Entries marked with "-" indicate no performance gain over the original learning rate. The values in parentheses represent the learning rate used.

Tuning initial value of α. We also investigate the effects of optimizing α_0 for DyT models, as presented in Table 14. Findings show only minor performance enhancements for select models when α_0 is tuned, indicating that the default initial value ($\alpha_0 = 0.5$) generally achieves near-optimal performance.

Model	LN	DyT ($\alpha_0 = 0.5$)	DyT (tuned)
ViT-B	82.3%	82.5%	82.6% ($\alpha_0 = 1.0$)
ViT-L	83.1%	83.6%	-
ConvNeXt-B	83.7%	83.7%	-
ConvNeXt-L	84.3%	84.4%	-
MAE ViT-B	83.2%	83.2%	83.4% ($\alpha_0 = 1.0$)
MAE ViT-L	85.5%	85.4%	-
DINO ViT-B (patch 16)	83.2%	83.4%	-
DINO ViT-B (patch 8)	84.1%	84.5%	-
DiT-B	64.9	63.9	-
DiT-L	45.9	45.7	-
DiT-XL	19.9	20.8	-
wav2vec 2.0 Base	1.95	1.95	-
wav2vec 2.0 Large	1.92	1.91	1.90 ($\alpha_0 = 1.0$)
HyenaDNA	85.2%	85.2%	-
Caduceus	86.9%	86.9%	-

Table 14 Impact of tuning the α_0 in DyT models. Optimizing α_0 from the default value ($\alpha_0 = 0.5$) yields only minor performance gains for select DyT models, implying the default initialization already achieves near-optimal performance. Entries marked with "-" indicate no improvement over the default α_0.

C Replacing Batch Normalization with DyT

We investigate the potential of replacing BN with DyT in classic ConvNets such as ResNet-50 (He et al., 2016) and VGG19 (Simonyan and Zisserman, 2014). Both models are trained on the ImageNet-1K dataset (Deng et al., 2009) using the training recipes provided by `torchvision`. The DyT models are trained using the same hyperparameters as their BN counterparts.

model	BN	DyT
ResNet-50	76.2%	68.9%
VGG19	72.7%	71.0%

Table 15 ImageNet-1K classification accuracy with BN and DyT. Replacing BN with DyT in ResNet-50 and VGG19 results in a performance drop, indicating that DyT cannot fully substitute BN in these architectures.

The results are summarized in Table 15. Replacing BN with DyT led to a noticeable drop in classification accuracy for both models. These findings indicate that DyT is struggling to fully replace BN in these classic ConvNets. We hypothesize this could be related to BN layers being more frequent in these ConvNets, where they appear once with every weight layer, but LN only appears once per several weight layers in Transformers.